High-Resolution NMR Determination of the Dynamic Structure of Membrane Proteins

Mariusz Jaremko[+], Łukasz Jaremko[+], Saskia Villinger[+], Christian D. Schmidt[+], Christian Griesinger, Stefan Becker, and Markus Zweckstetter*

Abstract: ^{15}N *spin-relaxation rates are demonstrated to provide critical information about the long-range structure and internal motions of membrane proteins. Combined with an improved calculation method, the relaxation-rate-derived structure of the 283-residue human voltage-dependent anion channel revealed an anisotropically shaped barrel with a rigidly attached N-terminal helix. Our study thus establishes an NMR spectroscopic approach to determine the structure and dynamics of mammalian membrane proteins at high accuracy and resolution.*

Human membrane proteins are responsible for a multitude of essential functions and are prime targets for the action of drugs. Rapid progress is being made in the structure determination of membrane proteins by X-ray crystallography and cryo-electron microscopy. However, ample evidence is mounting that information about the structure and dynamics of mammalian membrane proteins is required to understand their function.[1] Because NMR spectroscopy has access to both of these critical protein properties at physiologically relevant temperatures,[2] it can play a key role in this endeavor.

The challenge for NMR spectroscopy in studying the dynamic structure of membrane proteins lies in the sparsity of long-range structural information, because in high-molecular-weight systems, deuteration is compulsory. To compensate for the reduced number of NOE-based interproton restraints,

residual dipolar couplings (RDCs) are highly useful.[3] However, for large integral membrane proteins it can be difficult to prepare partially aligned NMR samples with sufficient quality and stability. Alternatively, relaxation enhancement induced by covalently attached paramagnetic spin labels can be valuable,[4] but distances derived from paramagnetic labels provide only rough estimates of the protein backbone fold.[5]

In this work, we address these limitations by exploiting the long-range order that is encoded in the nuclear magnetic spin relaxation of anisotropically tumbling macromolecules,[6] an approach that has not been applied to membrane proteins before. Through a combination of heteronuclear relaxation rates[6] and knowledge-based potentials,[7] we determined the solution structure and dynamics of the 283-residue human voltage dependent anion channel (hVDAC1)[8] at unprecedented resolution.

The two-dimensional ^1H-^{15}N TROSY[9] is the critical spectrum for the NMR-based analysis of detergent-solubilized membrane proteins. The high quality of this correlation map forms the basis for backbone resonance assignment and thus for the determination of the structure and dynamics of membrane proteins. Figure 1a shows the ^1H-^{15}N TROSY of the E73V mutant of hVDAC1, which shows decreased conformational exchange when compared to the wild-type protein[10] and good signal dispersion in LDAO micelles at 37°C (Figure 1a). Using TROSY-based triple-resonance experiments, we were able to sequence-specifically assign 92% of the backbone H^N, N, C^α, C′ resonances.[10b] On the basis of the experimental chemical shifts, the backbone torsion angles ψ, φ and the side-chain angle χ^1 were estimated (Figure S1 in the Supporting Information). In addition, HMQC-based ^{15}N-edited NOESY experiments provided 656 $^1H^N$-$^1H^N$ NOE-based medium- and long-range proton–proton distance restraints (Figure S2). The combined data were used for determination of the 3D structure of E73V hVDAC1. To this end, the structure was folded from an extended polypeptide with the help of a simulated annealing method implemented in Xplor-NIH[11] (subsequently referred to as Protocol 1; Table S1). The resulting ensemble of 20 lowest energy structures had a backbone r.m.s.d. of 2.5 Å (Figure 1b and Table S2). Similar to other NOE-based structures of hVDAC1,[10a, 12] the definition of the barrel shape and the conformation and position of the N-terminal helix could only be determined with modest accuracy (Figure 1b, Table S3, and Figure S3).

To improve the accuracy and precision of the E73V hVDAC1 coordinates and study its backbone dynamics, we performed ^{15}N spin-relaxation measurements at magnetic fields from 60 to 90 MHz nitrogen frequency. Because in these

[*] Dr. M. Jaremko,[+] Dr. Ł. Jaremko,[+] Dr. S. Villinger,[+] C. D. Schmidt,[+]
Prof. Dr. C. Griesinger, Dr. S. Becker, Prof. Dr. M. Zweckstetter
Max-Planck-Institut für Biophysikalische Chemie
Am Fassberg 11, 37077 Göttingen (Germany)
E-mail: Markus.Zweckstetter@dzne.de

Dr. Ł. Jaremko,[+] Prof. Dr. M. Zweckstetter
Deutsches Zentrum für Neurodegenerative Erkrankungen (DZNE)
Von-Siebold-Strasse 3a, 37075 Göttingen (Germany)

Prof. Dr. M. Zweckstetter
Department of Neurology
University Medical Center Göttingen, University of Göttingen
Waldweg 33, 37073 Göttingen (Germany)

[+] These authors contributed equally to this work.

⬚ Supporting information (including experimental details) for this article can be found under:
http://dx.doi.org/10.1002/anie.201602639.
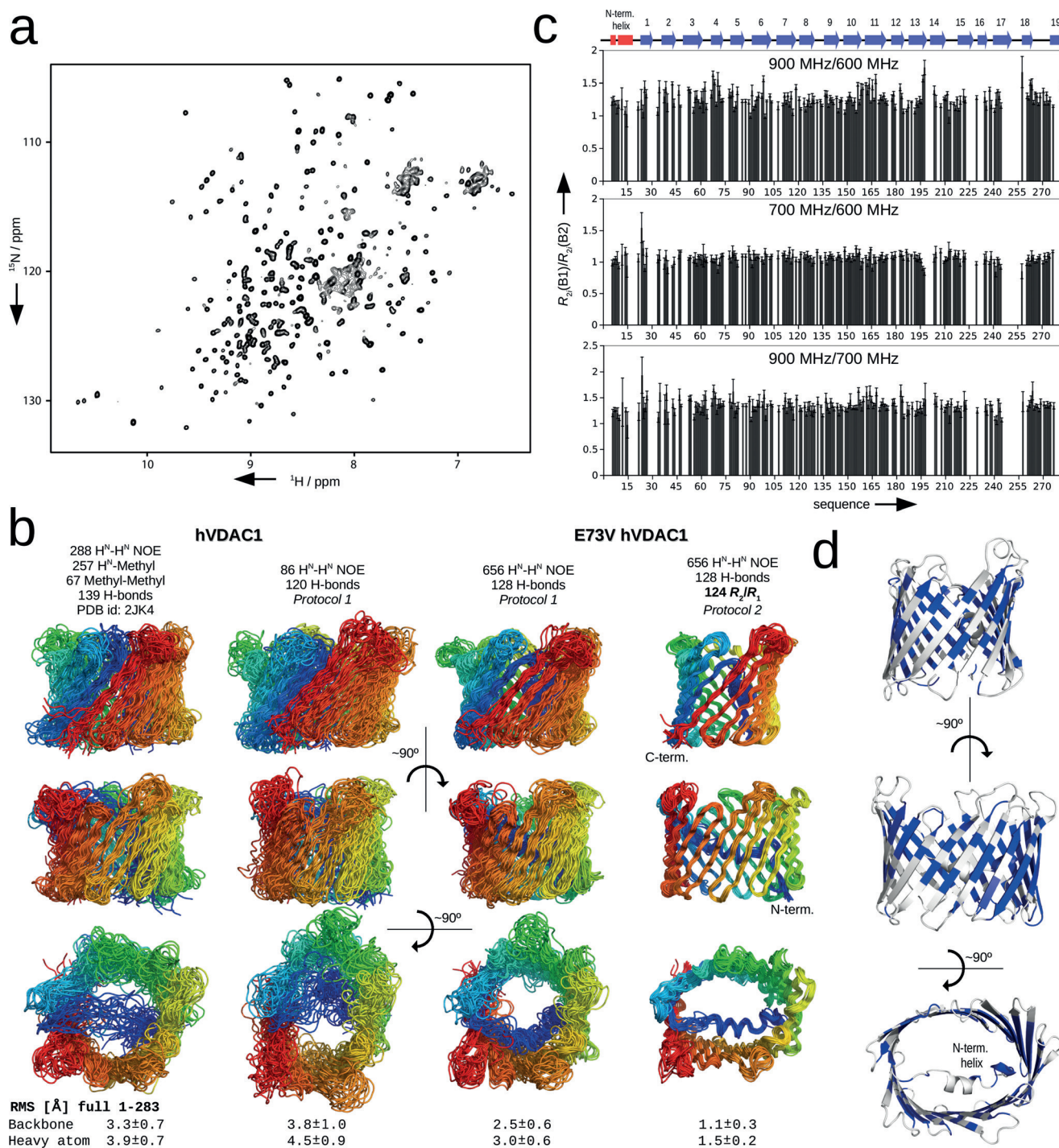
Figure 1. Dynamic and structural information encoded in ^{15}N spin-relaxation rates. a) 2D ^{1}H-^{15}N TROSY spectrum of the 283-residue E73V mutant of hVDAC1 in LDAO micelles recorded at 900 MHz. b) Gallery of NMR-based ensembles of the β-barrel of the human membrane protein VDAC1 (colored from the N- to the C-terminus from blue to red). From left to right: hVDAC1 structure reported in Ref. [12]; hVDAC1 structure calculated with the simulated annealing Protocol 1 on the basis of the NMR data reported in Ref. [10a]; E73V hVDAC1 structure derived from NMR data with Protocol 1; the ensemble of E73V hVDAC1, which was refined with Protocol 2 against the experimental ^{15}N-R_2/R_1 rates, shows a dramatic decrease in the spread of conformations. c) Residue-specific ratios of ^{15}N-R_2 relaxation rates [$R_{2i}(B_1)/R_{2i}(B_2)$] from three magnetic fields. Secondary motifs are shown as blue arrows (β-strands) and red rectangles (helix). Error bars show one standard deviation (SD). d) Lowest-energy conformation of E73V hVDAC1 refined against 124 ^{15}N-R_2/R_1 rates. Residues for which R_2/R_1 rates were used during structure refinement are shown in blue.

measurements the chemical shifts were encoded through the TROSY approach (Figure S4),[13] 537 pairs of high-quality R_1 and R_2 relaxation rates of the 32 kDa E37V hVDAC1 were obtained with average errors of 2.7% at 60 MHz, 3.1% at 70 MHz and 4.4% at 90 MHz (Figure 1c,d and Figure S5 and Tables S4, S5). The measurements at the three magnetic fields

were used to evaluate the overall quality of the data and to assess contributions from μs–ms motions. In addition, relaxation rates at multiple fields allow a more accurate determination of ps–ns motions.[2a] Analysis of the relaxation rates in the framework of the model-free approach (MFA)[14] demonstrated that most residues in the 19 β-strands of VDAC are rigid on the ps–ns time scale (Lipari–Szabo order parameter $S^2 > 0.85$ and correlation time for internal motions $\tau_i < 500$ ps; Figure S6).

Only a few residues in the N-terminal β-strands had elevated values for fast internal motion. In addition, no signs of chemical-exchange contribution to ^{15}N-R_2 rates were found (Figure 1c and analysis of relaxation rates by extended models for local motion; see the Supporting Information). The highest flexibility was observed in loops, in particular in the long loop between β-strands 18 and 19 (Figure S6), which is involved in binding to β-nicotinamide adenine dinucleotide.[12] Taken together, the analysis showed that protein motions can be determined with high accuracy in large membrane proteins with rotational correlation times reaching 40 ns.

The dependence of transverse and longitudinal relaxation rates on the rotational diffusion anisotropy of the protein provides information not only on internal motion but also on long-range structure.[6b] Because MFA analysis had shown that, in contrast to the wild-type protein,[10b] the E73V mutant of hVDAC1 is very rigid (Figure S6), we used its ^{15}N-R_2/R_1 rates for structure refinement. The selection of rigid residues with order parameters $S^2 > 0.85$, which are found mainly in secondary-structure elements, resulted in 124 residues with R_2 and R_1 values at three magnetic fields (i.e. $124*3 = 372$ R_2 rates and 372 R_1 rates, which corresponds to 744 experimental values in total). To extract the structural information encoded in the relaxation rates, the rotational correlation time (τ_c), the anisotropy (A) and the rhombicity (η) of the diffusion tensor have to be known a priori. These parameters were estimated by applying MFA analysis[14] to the NOE-based lowest-energy structure of E73V hVDAC1 (Table S6). To further test the impact of the initial coordinates for the estimation of diffusion-tensor parameters, the same analysis was repeated using the X-ray structure of mouse VDAC1 (mVDAC1; PDB ID: 3EMN,[15] Table S6). Subsequently, the structure of E73V hVDAC1 was refined against the experimental ^{15}N-R_2/R_1 rates. To this end Protocol 2 (Table S7) was designed, which makes use of the knowledge-based potentials torsionDB and HBDB,[7] which optimize the geometry of torsion angles and hydrogen bonds. The knowledge-based potentials narrow the conformational space to the physically most justified conformations as found among the highest-quality X-ray structures[16] and prevents overfitting of the orientational restraints, in particular in the case of outliers.[6b] As yet another check for the influence of diffusion-tensor parameters on the final coordinates, we varied the tensor parameters A and η, which were derived from the R_2/R_1-refined E73V hVDAC1 structure, by ±0.2 units and −50% and +100%, respectively. All calculations converged to highly similar 3D structures (Figure S7), which is in agreement with results from globular proteins and their complexes.[6,17]

The 3D structure of E73V hVDAC1, which was obtained through refinement against the experimental longitudinal and transverse NMR relaxation rates by using Protocol 2, which applies the above described knowledge-based potentials, is shown in Figure 1b, fourth column. The 20 lowest-energy structures fulfill the experimental distance and torsion-angle restraints and show improved Z-scores when compared to the starting structure (Figure S8 and Table S8). The ensemble tightly clusters around a single conformation, with a backbone r.m.s.d. of 1.1 Å for all 283 residues (Figure 1b). Each of the 19 β-strands was well defined and the N-terminal α-helix, which might play a role in VDAC gating,[8] was rigidly attached to the barrel wall (Figure 1b and 1d). The most flexible part of the structure was the linker, which connects the N-terminal helix to β-strand 1. When compared to the crystal structure of mVDAC1 (Figure 2a, blue structure), the
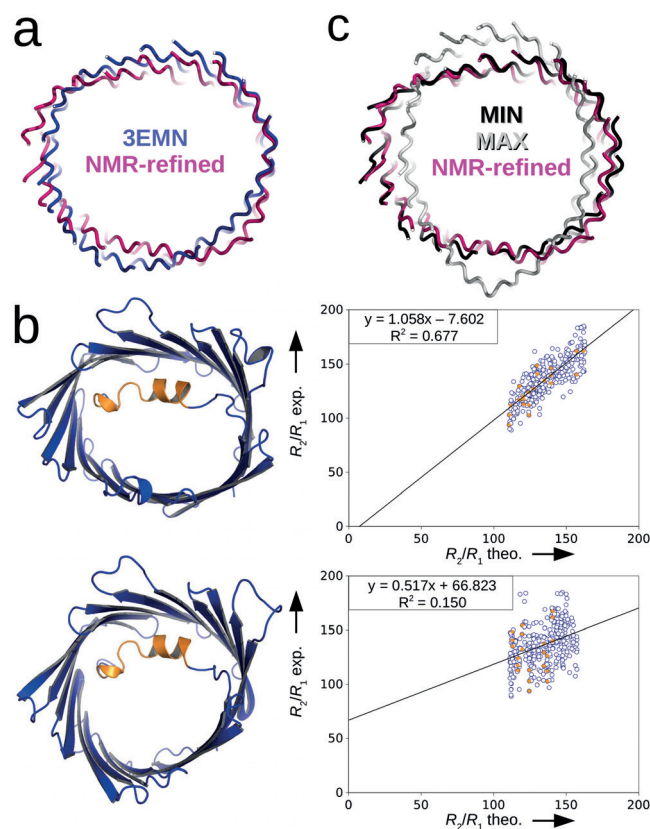
Figure 2. Validation of the high-resolution solution structure of E73V hVDAC1. a) Superposition of the 3D structure of E73V hVDAC1 refined against R_2/R_1 ratios (pink) with the crystal structure of mVDAC1 (PDB ID: 3EMN, blue).[15] The barrel of E73V hVDAC1, when viewed from above the membrane, has a more ellipsoidal shape. b) Correlation of experimental R_2/R_1 rates from three magnetic fields (scaled according to the theoretical field dependence) with values back-calculated from the crystal structure of mVDAC1 (PDB ID: 3EMN, lower panel) and the solution structure of E73V hVDAC1 (upper panel). The residues of the N-terminal helix together with the determined R_2/R_1 rates on the correlation plots are shown in orange. Experimental R_2/R_1 rates are in better agreement with the E73V hVDAC1 structure (see also Figure S9d). c) The barrel shape of E73V hVDAC1 (pink) is similar to one of the two maximum excursions (black and grey) observed in a 100 ns molecular dynamics trajectory of mVDAC1 embedded in a phospholipid bilayer.[10b]

barrel shape of E73V hVDAC1 (Figure 2 a, pink structure) is more anisotropic. This is a direct consequence of the experimental R_2/R_1 rates, because the R_2/R_1 rates fit better to the solution structure of E73V hVDAC1 than to the crystal structure of mVDAC1 (Figure 2 b and S9 d). The largest deviations between the experimental rates and values back-calculated from the X-ray structure of mVDAC1 were located in β-strands 9 and 10 (Figure S9). Notably, the ellipsoidal shape of E73V hVDAC1 as revealed by R_2/R_1 refinement is more similar (C$^\alpha$ r.m.s.d. of residues 26–283 = 2.1 Å) to an anisotropic barrel shape found during a 100 ns molecular dynamics trajectory of membrane-embedded mVDAC1 (Figure 2 c, black structure)[10b] than to the starting X-ray structure of mVDAC1 (C$^\alpha$ r.m.s. of residues 26–283 = 3.3 Å;[15] Figure 2 a, blue structure). This suggests that the E73V mutation and/or the micellar environment stabilize a conformation that the VDAC1 pore can adopt in a phospholipid bilayer according to molecular dynamics simulations. Notably, previous studies had shown that mutation of E73 affects hexokinase-I mediated VDAC gating and apoptosis inhibition.[18]

Protein motions generally complicate the interpretation of NMR data on the basis of a single conformation. This is true for relaxation rates as well as for other restraints such as NOEs and RDCs. When compared to the ^{15}N spin-relaxation rates, the use of RDCs for structure determination however is even more problematic, because RDCs are sensitive to dynamic events on a much wider timescale. As such, the proposed approach, that is, structure refinement on the basis of relaxation rates, has the unique advantage that both dynamic and structural information is obtained. Thus, flexible residues can be identified and excluded from structure refinement (as was done in the current application to VDAC). If a membrane protein is more dynamic, more residues will have to be excluded, but local regions might still benefit from refinement against the experimental ^{15}N-R_2/R_1 rates. In addition, ensemble calculations can be envisioned that make use of ^{15}N-R_2/R_1 rates and other NMR parameters.[19] In conclusion, we have established an NMR spectroscopic approach to determine the structure of membrane proteins at high accuracy and resolution.

[1] J. J. Liu, R. Horst, V. Katritch, R. C. Stevens, K. Wuthrich, *Science* **2012**, *335*, 1106–1110.
[2] a) A. G. Palmer 3rd, *Acc. Chem. Res.* **2015**, *48*, 457–465; b) A. K. Mittermaier, L. E. Kay, *Trends Biochem. Sci.* **2009**, *34*, 601–611.
[3] N. Tjandra, A. Bax, *Science* **1997**, *278*, 1111–1114.
[4] J. L. Battiste, G. Wagner, *Biochemistry* **2000**, *39*, 5355–5365.
[5] C. Klammt, I. Maslennikov, M. Bayrhuber, C. Eichmann, N. Vajpai, E. J. Chiu, K. Y. Blain, L. Esquivies, J. H. Kwon, B. Balana, U. Pieper, A. Sali, P. A. Slesinger, W. Kwiatkowski, R. Riek, S. Choe, *Nat. Methods* **2012**, *9*, 834–839.
[6] a) R. Bruschweiler, X. Liao, P. E. Wright, *Science* **1995**, *268*, 886–889; b) N. Tjandra, D. S. Garrett, A. M. Gronenborn, A. Bax, G. M. Clore, *Nat. Struct. Biol.* **1997**, *4*, 443–449.
[7] A. Grishaev, A. Bax, *J. Am. Chem. Soc.* **2004**, *126*, 7281–7292.
[8] V. Shoshan-Barmatz, V. De Pinto, M. Zweckstetter, Z. Raviv, N. Keinan, N. Arbel, *Mol. Aspects Med.* **2010**, *31*, 227–285.
[9] K. Pervushin, R. Riek, G. Wider, K. Wuthrich, *Proc. Natl. Acad. Sci. USA* **1997**, *94*, 12366–12371.
[10] a) M. Bayrhuber, T. Meins, M. Habeck, S. Becker, K. Giller, S. Villinger, C. Vonrhein, C. Griesinger, M. Zweckstetter, K. Zeth, *Proc. Natl. Acad. Sci. USA* **2008**, *105*, 15370–15375; b) S. Villinger, R. Briones, K. Giller, U. Zachariae, A. Lange, B. L. de Groot, C. Griesinger, S. Becker, M. Zweckstetter, *Proc. Natl. Acad. Sci. USA* **2010**, *107*, 22546–22551.
[11] C. D. Schwieters, J. J. Kuszewski, N. Tjandra, G. M. Clore, *J. Magn. Reson.* **2003**, *160*, 65–73.
[12] S. Hiller, R. G. Garces, T. J. Malia, V. Y. Orekhov, M. Colombini, G. Wagner, *Science* **2008**, *321*, 1206–1210.
[13] N. A. Lakomek, J. Ying, A. Bax, *J. Biomol. NMR* **2012**, *53*, 209–221.
[14] G. Lipari, A. Szabo, *J. Am. Chem. Soc.* **1982**, *104*, 4546–4559.
[15] R. Ujwal, D. Cascio, J. P. Colletier, S. Faham, J. Zhang, L. Toro, P. Ping, J. Abramson, *Proc. Natl. Acad. Sci. USA* **2008**, *105*, 17742–17747.
[16] G. A. Bermejo, G. M. Clore, C. D. Schwieters, *Protein Sci.* **2012**, *21*, 1824–1836.
[17] D. Fushman, R. Xu, D. Cowburn, *Biochemistry* **1999**, *38*, 10225–10230.
[18] H. Zaid, S. Abu-Hamad, A. Israelson, I. Nathan, V. Shoshan-Barmatz, *Cell Death Differ.* **2005**, *12*, 751–760.
[19] K. Lindorff-Larsen, R. B. Best, M. A. Depristo, C. M. Dobson, M. Vendruscolo, *Nature* **2005**, *433*, 128–132.